Environmental Research 244 (2024) 117945

Contents lists available at ScienceDirect

Environmental Research

journal homepage: www.elsevier.com/locate/envres

Effects of urban catchment characteristics on combined sewer overflows

Alessandro Farina [a,*], Rudy Gargano [b], Roberto Greco [a]

[a] Department of Engineering, University Luigi Vanvitelli, Aversa, 81031, Italy
[b] Department of Civil and Mechanical Engineering, University of Cassino and Southern Lazio, Cassino, 03043, Italy

ARTICLE INFO

Keywords:
Combined sewer overflow
Water pollution
Sensitivity analysis
Hydrological parameters
Urban catchments

ABSTRACT

Pollution from Combined Sewer Overflows (CSOs) cause diffuse environmental problems, which are still not satisfactorily addressed by current management practices. In this study, a sensitivity analysis was conducted on several CSO environmental impact indicators, with respect to parameters that characterise climate, urban catchment and the CSO structure activation threshold. The sensitivity analysis was conducted by running 10000 simulations with the Storm Water Management Model, using a simplified modelling approach. The indicators were calculated at yearly scale to evaluate overall potential effects on water bodies. The results could be used to estimate pollution load ranges, known the values of the input parameters, and to investigate suitable strategies to reduce pollution of the receiving water bodies. The percentage of impervious surface of the catchment was found the most influent parameter on all the indicators, and its reduction can contain the discharged pollutant mass. The activation threshold, instead, resulted the second least influent parameter on all the indicators, suggesting that its regulation alone would not be a suitable strategy to reduce CSO pollution. However, along with the reduction of the imperviousness, its increase could effectively decrease the concentration of pollutant in the overflow. The results also indicate that neither adopting sustainable urban drainage practices, nor interventions on the CSO device, significantly affect the frequency of the overflows. Therefore, restricting this latter was found to be ineffective for the reduction of both the discharged pollutant mass and the concentration of pollutant in the overflow.

1. Introduction

Combined Sewer Overflow (CSO) structures are hydraulic devices vastly used in combined sewer systems in many countries (Butler et al., 2018). Their presence in Urban Drainage Systems (UDSs) is fundamental as they prevent flooding, and overload of Wastewater Treatment Plant (WTP). Indeed, during heavy rainfall events, if the capacity of the sewers is exceeded, the mix of wastewater and stormwater would flood into the streets; also, an excessively diluted and highly variable influent would disrupt the WTP biological treatment processes (Trancone et al., 2022). CSO structures avoid these problems by diverting the overflow to water bodies through partition devices, such as transverse weirs, leap weirs, and side weirs. Ideally, an overflow occurs when $Q > DQ_W$, being Q the incoming flow, Q_W the mean wastewater discharge, and D a dilution threshold.

However, CSOs may cause short- or long-term environmental problems to water bodies (Butler et al., 2018) and to public health (McGinnis et al., 2022; Sojobi and Zayed, 2022), such as dissolved oxygen depletion, eutrophication, toxicity, and recreational sites interdiction. These problems arise because the untreated overflow may contain high levels of pollutants, due to the insufficient dilution of the sewage or the washoff of sediments accumulated on the catchment surface (Tu and Smith, 2018) or in the sewers (Seco et al., 2018). This issue occurs especially in the early part of the runoff and the phenomenon is commonly referred to as the first-flush (Barco et al., 2008; Gupta and Saul, 1996; Mamun et al., 2020), although more complex site-specific flush dynamics patterns are receiving increasing attention in recent literature (e.g., Jensen et al., 2022). The transported pollutants may origin from dirt, debris, or suspended solids (Ferraro et al., 2023), and they can be organic matter (Seidl et al., 1998), heavy metals (Xu et al., 2018), toxic compounds (Nickel and Fuchs, 2019), drugs (Munro et al., 2019), microplastics (Di Nunno et al., 2021; Yaranal et al., 2023), or emerging contaminants (Petrie, 2021).

In literature, the evaluation of pollution from CSOs is usually carried out from a case study perspective (Botturi et al., 2021; Sandoval et al., 2013), making the results hardly extendable to different CSO locations

* Corresponding author.
E-mail address: alessandro.farina@unicampania.it (A. Farina).

https://doi.org/10.1016/j.envres.2023.117945
Received 17 August 2023; Received in revised form 11 December 2023; Accepted 12 December 2023
Available online 16 December 2023

and different UDSs. Indeed, there is a lack of generalised methods to assess pollutant loads from CSOs, which would be more widely applicable to different UDSs. An example of such a method is presented in Dirckx et al. (2022), for which, however, water quality measurements from samples collected at the CSO structure are required, which are rarely available.

Hence, given the uncertainty of water quality modelling in UDSs (Jia et al., 2021), and the scarcity of reliable CSO water quality monitoring data (Schellart et al., 2023), most studies focused on overflow volume reduction (e.g., Dirckx et al., 2019; Eulogi et al., 2022; Joshi et al., 2021; Lucas and Sample, 2015; Torres et al., 2022; Vezzaro, 2021; Zhang et al., 2023). Nevertheless, the volume does not carry information on pollutant concentration and mass. Few studies, instead, investigated other indicators, like pollutant mass (e.g., Pistocchi, 2020; Romero et al., 2021) or event duration (Quaranta et al., 2022), unfolding the necessity of further research also in this direction.

CSO regulation also has some flaws. To ensure sufficient dilution in the receiving water body, many European countries adopted standard values for the dilution coefficient, D, nationwide (Zabel et al., 2001), and to date, most of them enforce further limitations on simplistic indicators, such as the number of overflows per year (Botturi et al., 2021). However, evidence showed that CSO structure design criteria are more linked to the WTP capacity (Dirckx et al., 2011), and to protect infrastructures under peak dry weather flow conditions (Giakoumis and Voulvoulis, 2023), rather than to environmental protection. Additionally, Engelhard et al., 2008 found that the number of overflows per year has no influence on the receiving water body quality.

Under this scenario, it would be useful to assess the CSO environmental impact variability, by means of effective pollution indicators, with the final aim of choosing which overflow events to permit. Indeed, designing CSO structures with a highly precautionary approach avoids the discharge of pollutants in the receiving water body, but makes the WTP operation more difficult. Viceversa, protecting WTPs towards heavy rainfall events requires a less stringent CSO structure design approach, that leads to greater pollution load discharged. Also, an effective study about the CSO damages on water bodies (Sojobi and Zayed, 2022) requires to be conducted over long periods to evaluate overall effects, and not only those related to single events.

This study presents a method to estimate the variability of CSO quantity and quality, that allows to analyse the effects, at yearly scale, of different parameters characterising the local rainfall, the urban catchment, and the CSO structure, on overflows.

The proposed method was used to conduct a robust Sensitivity Analysis (SA) on 10000 sets of the above-mentioned parameters. Therefore, this approach is valid for a wide range of case studies and could be valuable especially when accurate CSO quantity and quality measurements are not available. The results of the SA allowed to find the most significant parameters affecting CSOs, and they are suitable to plan strategies to effectively reduce pollution loads. If the vulnerability of the receiving water body is also known, this method could be used to assess the impact of those strategies and reach target levels of pollution reduction.

Also, to provide a practical example of application of the proposed method, CSO pollutant loads were evaluated for a real case study in the city of Portici (Italy).

Lastly, some finds of this study can be useful to support CSO regulation improvement.

2. Materials and methods

An approach to evaluate the variability of CSO environmental impact indicators (EIIs), at yearly scale, was developed to estimate overall pollution effects, for UDSs with different characteristics. Therefore, a large set of hypothetical UDSs (10000) were simulated, having different sets of hydrological and geomorphological parameters of the urban catchment (UC) and different features of the CSO structure. This analysis allows to evaluate the pollution load being discharged into water bodies.

The quantitative and qualitative variability of CSOs depends on climate forcing, characteristics of the UDS, and pollution in sewer discharge. In particular, the following aspects were investigated:

- The rainfall regime, which is correlated with CSO volume (Farina et al., 2022; Sandoval et al., 2013; Schroeder et al., 2011).
- Different land-uses, which lead to different ratios between the runoff generated by the rainfall and the water retained by the urban catchment.
- The morphology of the UC, which leads to different hydrologic responses to the rainfall input.
- The water supply and use, and the population density, which determine the wastewater discharge, Q_W, in turn determining the mass of pollutants deriving from sanitary flow during CSOs.
- Local regulations, which determine the CSO structure activation threshold.

Four main steps were taken (Fig. 1), briefly presented below and expanded in the next sub-sections:

1. A simplified hydrological and quality model was adopted for the assessment of UDS response and of the CSO structure operation.
2. Parameters pertaining the rainfall, the UDS and the CSO structure, with the highest expected influence on hydrograph and CSO volume, were selected. Their ranges of variability were defined based on typical characteristics of urban environments and current CSO regulations.
3. Suitable EIIs were identified. Besides the volume and the frequency of the overflows, also the mass and concentration of pollutant in the overflows were considered.
4. A sensitivity analysis was conducted, searching for meaningful relationships between the parameters and the EIIs: the Spearman correlation coefficients were calculated for each pair of parameters and EIIs.

The SA involved a wide numerical investigation on the different parameters, through analysing 10000 hypothetical UDSs: each model run for a UDS consisted in the simulation of one year, sampled from the available 20 years.

Finally, an application example of the use of the SA results was developed for an actual UDS in the city of Portici (Italy).

2.1. Simplified modelling approach

A specific modelling approach for the robust estimation of quantity and quality of CSOs was developed, and it consisted in two simplified models: the UDS with the CSO structure, and the water quality. This approach was used in this study to conduct the SA, but it could be used, more generally, in planning studies which do not require a detailed simulation of the hydraulics and the transport of pollutants in single sewer conduits, but rather global estimations at the CSO structure location. The robustness of the method comes from the few parameters required by the simplified models.

2.1.1. UDS and CSO structure model

A hydrological lumped model of a hypothetical UDS with a CSO structure (Fig. 2) was modelled in the Storm Water Management Model (SWMM). SWMM was used for its flexibility and its ability to work with Python interfaces, like *swmm-api* (Pichler, 2022), used in this study.

More precisely, SWMM uses a nonlinear reservoir conceptual model (Chen and Shubinski, 1971) for the assessment of the runoff from the pervious and the impervious surface, which is calculated as qA, where q and A are the runoff per unit area, and the area, respectively for both the surfaces (Equation 1). The total runoff is then the sum of the runoff from both the surfaces.

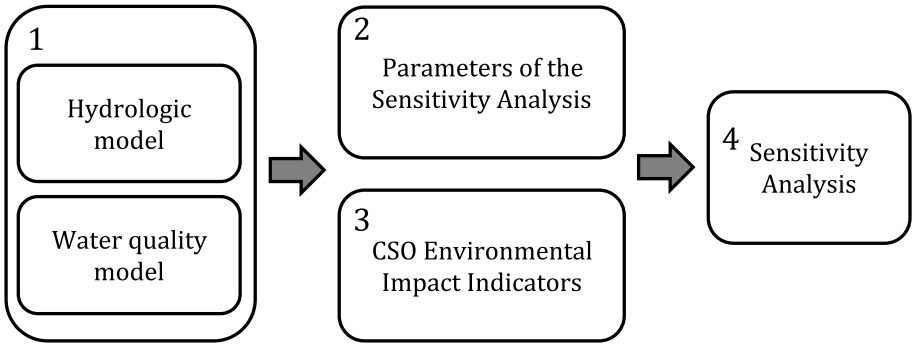

Fig. 1. Flowchart of the sensitivity analysis approach.

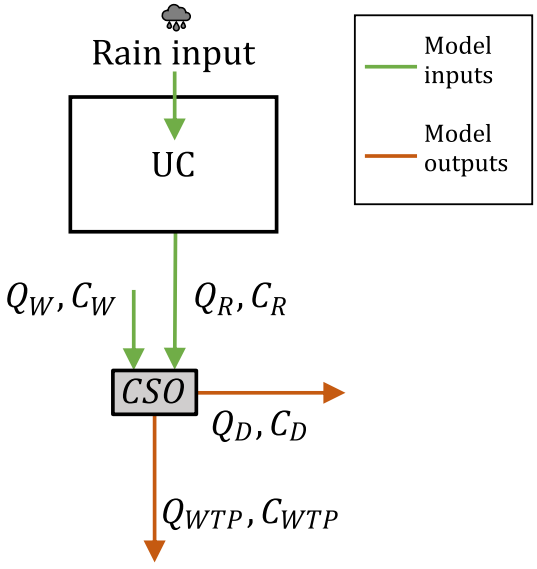

Fig. 2. Sketch of the model of the UDS and the CSO structure. The stormwater runoff, Q_R, and the outputs, were calculated running SWMM simulations.

$$q = \frac{W\sqrt{s}}{An}(d - d_s)^{5/3} \tag{1}$$

In Equation 1, W is the width of the catchment (Rossman and Huber, 2016a), s is the slope, n is the Manning roughness coefficient of the pervious/impervious surfaces, d is the depth of the water accumulated over the surface, resulting from the rainfall, and d_s is the height of the depression storages of the pervious/impervious surfaces. Equation 1 can also be written as:

$$q = \alpha(d - d_s)^{5/3} \tag{2}$$

where $\alpha = \frac{W\sqrt{s}}{An}$ is the nonlinear reservoir constant. Hence, the following equation can be used for α:

$$\alpha = \frac{f^W\sqrt{s}}{n\sqrt{A}} \tag{3}$$

where $f^W = \frac{W}{\sqrt{A}}$ is a shape coefficient which expresses how the UC shape differs from a square.

As in Farina et al. (2023), the UDS was schematised through a single catchment, the parameters of which can be assigned from cartographic information, and the hydraulics of the sewer network was not computed. Thus, this approach directly estimates the discharge of the UC, through a hydrological model. This approach had been tested against several real UDSs and had been shown to provide reliable predictions of hydrograph at the outlet (in terms of Nash-Sutcliffe Efficiency) and CSO volume (Farina et al., 2023). The sketch of the hydrological model is represented in Fig. 2.

The CSO structure operation is represented with an ideal cut-off behaviour, so that overflows occur when $Q_R + Q_W > DQ_W$ (see Fig. 2), being Q_R the stormwater runoff, Q_W the wastewater discharge, and D the dilution threshold, thus the overflow Q_D is calculated as

$$Q_D = Q_R + Q_W - Q_{WTP} \tag{4}$$

and the flow conveyed to the WTP is a fixed value $Q_{WTP} = DQ_W$.

The inputs of the SWMM model (Fig. 2) were Q_W, the rainfall timeseries, and the concentration of pollutant in the wastewater and in the stormwater, respectively C_W and C_R. The outputs of the SWMM model (Fig. 2) were the overflow, Q_D, the pollutant concentration in the overflow, C_D, and the pollutant concentration in the flow conveyed to the WTP, C_{WTP}. The definition of C_W and C_R is presented in the next section.

2.1.2. Water quality model

The Biochemical Oxygen Demand after five days, BOD_5, which is a common index of organic water pollution (Sawyer et al., 2003), was assumed as an example water quality parameter. The methodology can also be extended to other pollution indices.

Typical values for the BOD_5 concentration in wastewater, C_W, are broadly available in literature (Butler et al., 2018; Inc. Metcalf & Eddy, 2013), and here, a plausible value $C_W = 250\,\frac{\text{mg}}{\text{L}}$ was used.

The proposed model assumes the perfect mix between Q_W and Q_R, hence the concentration of pollutant in the overflow, C_D, is the weighted average between the concentration in the wastewater, C_W, and the concentration in the stormwater, C_R.

To calculate C_R, the BOD_5 dynamics were modelled through classical build-up and wash-off functions (Butler et al., 2018; Rossman and Huber, 2016b), assuming that the pollutant accumulation over the ground surface, during dry periods, follows an exponential law:

$$b(t_b) = C1\left(1 - e^{C2 \cdot t_b}\right) \tag{5}$$

where $b(t_b)$ is the pollutant mass per unit area, t_b represents the antecedent dry weather duration (in days), $C1$ is the maximum mass of pollutant per unit area of the urban surface, and $C2$ is a growing rate constant. Then, during rainfall events, the pollutant is washed off the surface with an exponential law:

$$w(t_w) = b_0 e^{-C3\ q^{C4} t_w} \tag{6}$$

where $w(t_w)$ is the washed pollutant mass per unit area, t_w represents the elapsed time (in days) from the beginning of the wash-off, b_0 is the mass of pollutant per unit area on the catchment surface at the beginning of the wash-off, $C3$ and $C4$ are wash-off coefficient and exponent, and q is the runoff per unit area.

In literature, estimations of $C1$, $C2$, $C3$, $C4$ are available for the Total

Suspended Solids, *TSS*, (e.g., Hossain et al., 2010; Tu and Smith, 2018; Wicke et al., 2012), which is the most analysed water quality parameter (Maniquiz-Redillas et al., 2022). Here, average values were retrieved from literature, thus $C1 = 25\frac{kg}{ha}$, $C2 = 0.25\,days^{-1}$, $C3 = 0.25\,mm^{-1}$, and $C4 = 0.9$ were assumed. Since different pollutants are strictly correlated to *TSS* (Mallin et al., 2009; Nasrabadi et al., 2016), the values of the parameters $C2$, $C3$, and $C4$ were considered suitable also for the simulation of the BOD_5; differently, assuming 0.4 as the average of the $\frac{BOD_5}{TSS}$ fraction values observed in UDSs in studies analysing stormwater runoff (Fig. 3) (Barco et al., 2008; Luo et al., 2009; Nazahiyah et al., 2007; Zeng et al., 2019), $C1 = 0.4{\cdot}25\frac{kg}{ha} = 10\frac{kg}{ha}$ was used for the BOD_5.

2.2. Parameters

The variability of CSOs in an UDS of fixed area $A = 1km^2$, was analysed towards the following independent parameters (summarised in Table 1, along with their investigated ranges), through the sensitivity analysis:

- Twenty years of rainfall depth timeseries, at 10 min resolution, were used as the weather forcing. Since in Section 4.2 the results of the SA are also applied to the example of a real case study in Portici, Italy (Fig. 4), the rain gauge of Ercolano, the nearest to Portici, was used to collect rain data (DPCN, 2023). The recorded timeseries (from 2003 to 2022) had $< 1\%$ of missing/incorrect data. The yearly cumulated rain, R_D, varied in the range $[676; 1170]$ mm, the maximum daily cumulated rain varied in the range $[33; 132]$ mm, the maximum intensities were in the range $[50; 122]\frac{mm}{hr}$, with yearly rainy days varying in the range $[78; 149]$ days.
- Wastewater production per unit area, V_W. Its range was calculated considering values of population (p) density in the range $[3000; 8000]\frac{p}{km^2}$, $250\frac{L}{day}$ of water per capita, and 0.8 as the ratio of the delivered water being conveyed to the sewer system after use. The resulting range for the yearly V_W was $[200; 600]$ mm.
- Percentage of impervious surface, I. In urban areas, I can vary broadly, depending on the surface characteristics. Hence, I was analysed in the range $[30; 90]\%$.
- Nonlinear reservoir constant, α (defined in Section 2.1.1), varied (for the impervious surfaces) in the range $[5; 700]{\cdot}10^{-4}\frac{m^{-2/3}}{s}$, resulting from the assumed ranges of f^W, $\left[\frac{1}{4}; 4\right]$, s, $[0.5; 5.0]\%$, and n, $\left[\frac{1}{30}; \frac{1}{80}\right]\frac{s}{m^{1/3}}$; this latter range was used for the impervious surfaces, while a constant value of $\frac{1}{10}\frac{s}{m^{1/3}}$ was used for the Manning coefficient of the pervious surfaces.
- Threshold dilution coefficient, D. Its values, adopted by European Countries, can be found in Zabel et al. (2001). In this study, D varied in the range $[3; 9]$.

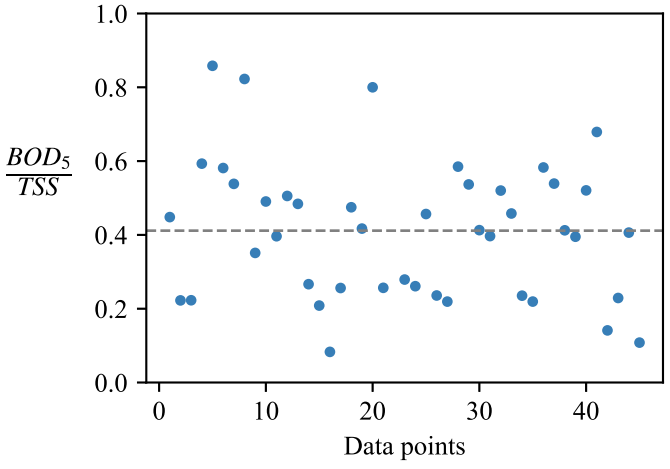

Fig. 3. $\frac{BOD_5}{TSS}$ fraction during storm runoff in urban areas, from Barco et al. (2008); Luo et al. (2009); Nazahiyah et al. (2007); Zeng et al. (2019). The average value of 0.4 was assumed in this study.

The variability of CSOs was also analysed towards the derived hydrological parameter $\frac{R_D}{V_W}$, varying in the range $[1.13; 5.85]$.

2.3. CSO environmental impact indicators

The potential environmental damages of CSOs depend on their characteristics, and on the vulnerability of the water bodies. In this study, we explored only the former, by defining suitable environmental impact indicators, EIIs, listed below:

- The frequency of activation, F, expressed as the number of overflows.
- The discharged volume, V, expressed as volume per unit area A of the urban catchment.
- The discharged pollutant mass, M, calculated as the product between the concentration of pollutant in the overflow and the discharged volume.
- The average concentration of pollutant, C_D, in the overflow, Q_D.

The EIIs were evaluated at yearly scale, from the model outputs, running extended period simulations of the proposed model (see Section 2.1). For the computations, a CSO starts when $Q_{D_i} = 0$ and $Q_{D_{i+1}} > 0$, and ends when Q_D becomes again zero, followed by the establishment of dry weather flow conditions in the conduit, namely when $Q_{R_i} > 0$ and $Q_{R_{i+1}} = 0$ (Fig. 5). As illustrated in Fig. 5, the choice of the time resolution of the simulations may affect the estimated duration of CSOs, as well as the corresponding discharged volumes and pollutant mass. In this study, a time step $\Delta t = 10$ min has been adopted, as it allows to contain the error in the evaluation of CSOs.

F is the number of CSOs in a year, while the other EIIs were calculated as follows:

$$V = \sum_{i=1}^{N} Q_{D_i} \Delta t \Big/ A \tag{7}$$

$$M = \sum_{i=1}^{N} C_{D_i} Q_{D_i} \Delta t \tag{8}$$

$$C_D = \frac{\sum_{i=1}^{F} C_{D_i}}{F}, \text{ with } C_{D_i} = \frac{M_{event}}{V_{event}} \tag{9}$$

being $N = \Delta T / \Delta t$, where $\Delta T = 1$ year, and Δt is the resolution of the model output timeseries. In this study $\Delta t = 10$ min was adopted, corresponding to $N = 52560$ time steps per year. As anticipated in Section 2.1.2, M and C_D were evaluated for the BOD_5.

2.4. Sensitivity analysis

A Sensitivity Analysis, SA, allows studying the variability of output variables upon variations of different input parameters, finding the inputs mostly affecting each output (Saltelli et al., 2008, 2010). Commonly, a SA includes:

- Sampling the space of the SA input parameters.
- Running model simulations associated with the sampled sets of values.
- Analysing the dependence of the SA outputs upon the SA inputs.

Here, the SA inputs are the parameters (Table 1), and the SA outputs

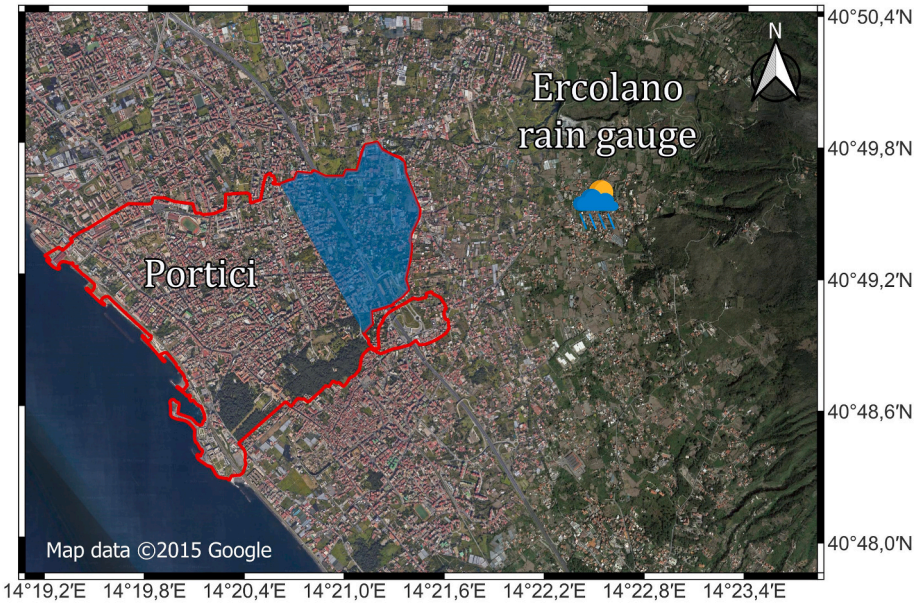

Fig. 4. Location of Portici (Italy) and the rain gauge of Ercolano. An example of use of the sensitivity analysis was developed in Section 4.2, for the catchment highlighted in blue, with $A = 1\ km^2$, for which the geo-morphological characteristics of the urban catchment were known.

Table 1
Parameters used for the Sensitivity Analysis.

Sensitivity Analysis parameter	Description	Range
R_D [mm]	Yearly rainfall depth	[676; 1170]
V_W [mm]	Yearly wastewater production	[200; 600]
I [%]	Percentage of impervious surface	[30; 90]
$\alpha = \frac{f^W\sqrt{s}}{n\sqrt{A}}\left[\frac{\mathrm{m}^{\frac{2}{3}}}{\mathrm{s}}\right]$	Nonlinear reservoir constant	[5; 700]·10^{-4}
D [−]	Dilution threshold	[3; 9]

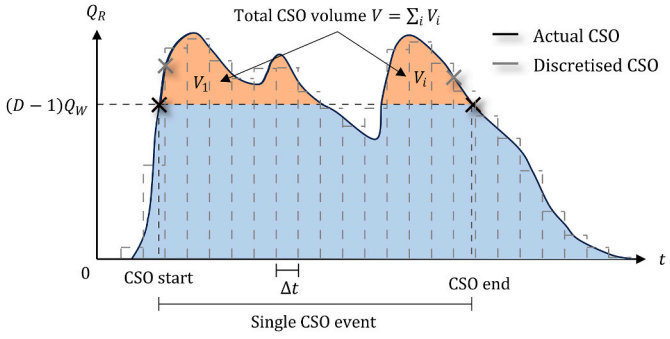

Fig. 5. CSO definition: an overflow starts when $Q_{D_i} = 0$ and $Q_{D_{i+1}} > 0$, and ends when Q_D becomes again zero, followed by the establishment of dry weather flow conditions in the conduit, namely when $Q_{R_i} > 0$ and $Q_{R_{i+1}} = 0$. The time resolution of the simulations was $\Delta t = 10\ min$.

are the environmental impact indicators, EIIs (F and Equations 7-9)). Specifically, 10000 values were randomly generated from each range of the independent parameters (i.e., R_D, V_W, I, α, D), therefore a 10000 × 5 matrix was obtained. For the generation, a uniform distribution of the values in each range was assumed, in absence of further knowledge on their frequency distribution. Thus, each row of the matrix is a set of input parameters of the hydrological model.

For each set, a model simulation with the corresponding parameters was run, and the outputs were stored and used to calculate the EIIs.

The Spearman rank (r) correlation coefficient, $S_{X,Y}$, was used to measure the influence of a parameter (X) on each EII (Y):

$$S_{X,Y} = \frac{cov(r(X), r(Y))}{\sigma_{r(X)}\sigma_{r(Y)}} \tag{10}$$

$S_{X,Y}$ is more suitable than the Pearson correlation coefficient to assess non-linear relationships, as it measures the linear correlation between the ranks of the variables. To check if any of the studied EIIs were redundant, the $S_{Y,Y}$ were also calculated among all the EIIs.

3. Results

The environmental impact indicator, EIIs, showed different sensitivity to the parameters considered in this study, suggesting that some of them are more influent than others in evaluating the CSO environmental impact on water bodies. Different correlations emerged among the EIIs: in Fig. 6, the matrix of the Spearman correlation coefficients, $S_{Y,Y}$ (Equation 10), for all the EIIs, is represented.

For example, the pollutant concentration in the overflow, C_D, decreases when the discharged volume, V, increases ($S_{C_D,V} = -0.77$), while the discharged pollutant mass, M, increases when V increases

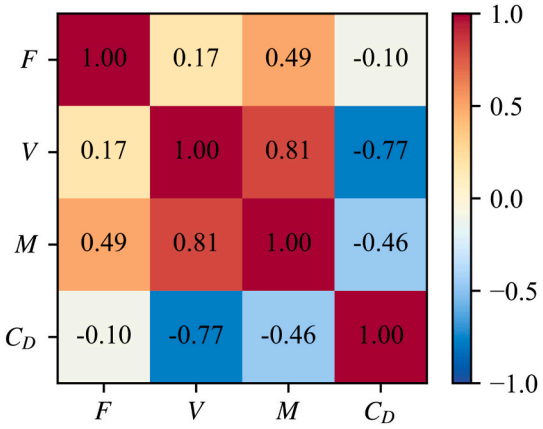

Fig. 6. Spearman correlation coefficients, $S_{Y,Y}$, of the environmental impact indicators, EIIs.

($S_{M,V} = 0.81$). It would be expectable that also M and C_D are correlated, but this was not entirely confirmed by the results, since $S_{M,C_D} = -0.46$ indicates only a moderate correlation. This suggests that, when M is known, it is not straightforward to derive C_D, and vice versa, and also that the dilution effect due to the increased discharged volume tends to prevail on the increase of discharged pollutant mass. Finally, the frequency of the CSOs, F, resulted only moderately correlated with M ($S_{M,F} = 0.49$), and totally uncorrelated with C_D ($S_{C_D,F} = -0.10$), and with V ($S_{V,F} = 0.17$), suggesting that it is not possible to assess any of the CSO characteristics through F alone.

3.1. Sensitivity of the EIIs

In Fig. 7, the EIIs are plotted against the parameters, to visually investigate the existence of meaningful relationships: each plot has 10000 points, corresponding to all the simulations.

For a given pair of X, Y variables, the relevant scatter plot represents the variability of an EII associated to a parameter: if the points are highly dispersed and do not show a clear trend, the considered EII is sensitive to other parameters, and, equivalently, that parameter is not the primary source of its variability. The red lines fit the scatter plots of the X, Y pairs through a power-law curve, $Y = aX^b$, and their thickness is proportional to $|S_{X,Y}|$: if the red line is barely visible, the $|S_{X,Y}|$ value is low. This is the case, for example, of the plot of the wastewater production, V_W, versus the overflow pollutant concentration, C_D, which relationship has the lowest $|S_{V_W,C_D}| = 0.04$, showing that those two variables were definitely not correlated. In Fig. 8, the matrix of the correlation coefficients, $S_{X,Y}$, for each pair of X, Y variables, is represented.

Instead, if the points are dense and clearly exhibit a positive or negative trend, the variability of the considered EII is highly due to that parameter, and, equivalently, that parameter is the primary source of variability of the EII. In this case, the red line is thick and clearly visible. This is the case, for example, of the plot of the percentage of impervious surface, I, versus the discharged volume, V, which relationship had the highest $|S_{I,V}| = 0.83$. Therefore, the plots having high density of points, and thick fitting lines, show the most significant relationships between the parameters and the EIIs. In Table 2, EII statistics are given.

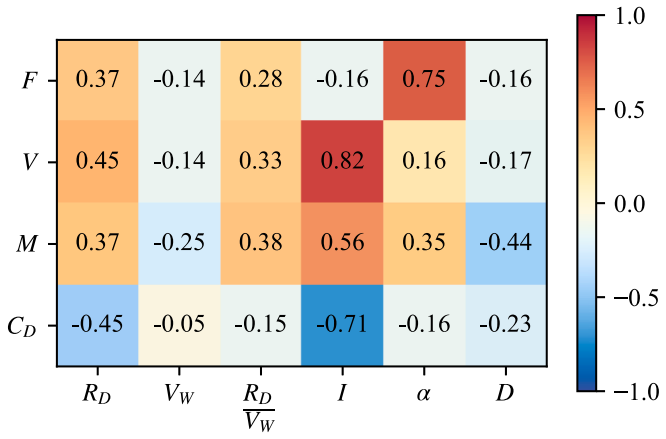

Fig. 8. Spearman rank correlation coefficients, $S_{X,Y}$, of each pair of parameter and EII.

Table 2
EII statistics, evaluated for 10000 one-year simulations, each with a different set of parameter values sampled in the assumed ranges.

Environmental Impact Indicator	Minimum	Maximum	Mean
F [−]	17	192	89
V [mm]	37	905	393
M [kg]	3794	31309	19156
C_D $[\frac{mg}{L}]$	55	154	97

For a given parameter, the sum of the $|S_{X,Y}|$ of all the EIIs can be an indicator of its overall influence on all the EIIs. On this basis, I resulted the most influent ($\sum_Y |S_{I,Y}| = 2.25$), while V_W was the least influent ($\sum_Y |S_{V_W,Y}| = 0.58$). The same summations, for all the parameters, are given in Table 3.

Likewise, for a given EII, the sum of the $|S_{X,Y}|$ of all the parameters,

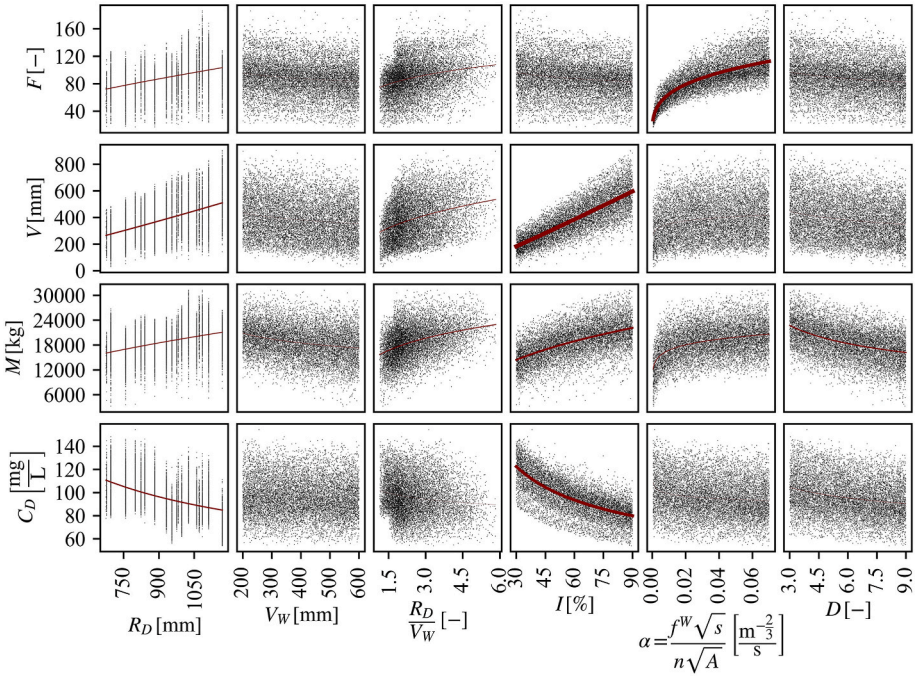

Fig. 7. Scatter plots of each pair of parameters (on the X axis) and EII (on the Y axis). The thickness of the red lines, that fit the X, Y points, is proportional to the absolute value of the Spearman correlation coefficients, $|S_{X,Y}|$, of Fig. 8.

Table 3
On the first two columns, the sum of the $|S_{X,Y}|$ of all the EIIs are shown, representing the overall influence of each parameter; the parameters are sorted by decreasing influence on the EIIs. On the last two columns, the sum of the $|S_{X,Y}|$ of all the parameters are shown, representing the sensitivity of each EII; the EIIs are sorted by decreasing sensitivity.

Parameter (X)	$\sum_Y \lvert S_{X,Y}\rvert$	Environmental Impact Indicator (Y)	$\sum_X \lvert S_{X,Y}\rvert$
I	2.25	M	2.35
R_D	1.64	V	2.07
$\alpha = \frac{f^W\sqrt{s}}{n_i\sqrt{A}}$	1.42	F	1.85
$\frac{R_D}{V_W}$	1.15	C_D	1.75
D	1.00		
V_W	0.58		

can be an indicator of its overall sensitivity to all the parameters. On this basis, M was the most sensitive ($\sum_X |S_{X,M}| = 2.35$), while C_D was the least sensitive ($\sum_X |S_{X,C_D}| = 1.75$). The same summations, for all the EIIs, are also given in Table 3.

3.2. Most significant relationships

Among the twenty-four calculated correlations between the parameters and the indicators, EIIs, (Figs. 7 and 8), seven of them showed $|S_{X,Y}| \geq 0.40$ (they are listed in Table 4), while only three of them showed $|S_{X,Y}| \geq 0.70$.

With the aim of mitigating the CSO impact on water bodies, it is interesting to explore which parameters of the UDS or of the CSO structure can be adjustable through design choices that could lead to significant reduction of CSOs, i.e., inducing valuable variations of the EIIs. Hereafter, those parameters are defined as *controllable*, while the other ones are called *non-controllable*.

Indeed, for an UDS with fixed area (in this study $A = 1$ km^2 was assumed), not all the parameters are *controllable*. The yearly rainfall depth, R_D, the wastewater production, V_W, and their ratio $\frac{R_D}{V_W}$, are *non-controllable*, as R_D depends on the climate, and V_W depends on the population density. The nonlinear reservoir constant, α (Equation 3) is *non-controllable* as well, as it depends on the morphologic characteristics of the urban catchment, UC: its shape (through f^W), its mean slope s, its area A, and the Manning coefficient, n. Only n could be controlled in the formula of α, by changing the roughness of the paved surfaces throughout the catchment: however, n conceptually encompasses the hydraulic resistance encountered by draining water along its path, not only above the ground surface but also through secondary elements of the drainage system. Hence, even diffuse interventions on the pavements would not significantly affect its value.

Thus, it is worth looking at the most significant relationships regarding the *controllable* parameters, namely the percentage of impervious surface, I, and the dilution coefficient, D. Those relationships and their relevant $S_{X,Y}$ coefficients are listed in Table 5, in which the equations of their fitting lines (Fig. 7) are also given. In particular:

- I can be reduced by increasing green areas in urban environments, for example substituting impervious pavements with permeable ones (e.g., in parking lots), or implementing other sustainable urban drainage strategies (for example installing green roofs, planting shrubs and trees, or building rain gardens).
- D can be set as a design parameter of the CSO structure. For example, for side weirs, it is possible to modify the height of the weir crest, or, for leap weirs, it is possible to change the width and the shape of the orifice.

Table 4
Most significant correlations between parameters and EIIs, and their $S_{X,Y}$ value. The table is sorted in decreasing order of $|S_{X,Y}|$.

Correlation	$S_{X,Y}$
I vs V	0.82
α vs F	0.75
I vs C_D	− 0.71
I vs M	0.56
R_D vs V	0.45
R_D vs C_D	− 0.45
D vs M	− 0.44

4. Discussion

The EIIs, which express the potential environmental impact of CSOs on water bodies, showed different dependence with respect to *controllable* and *non-controllable* parameters. In particular, the discharged volume, V, the overflow pollutant concentration, C_D, and the discharged pollutant mass, M, could be reduced, if strategies to adjust the percentage of impervious surface, I, or the dilution threshold, D, are designed, as described below; instead, the frequency of overflows, F, is hardly *controllable* as it depends mostly on the nonlinear reservoir constant, α, as described in Section 4.1.

Fig. 9 shows the influence of I and D, on M and C_D. M can be reduced by decreasing I (Equation 13), and this would also reduce V (Equation 11), but at the same time it would increase C_D (Equation 12) and the volume conveyed to the WTP, V_{WTP}, due to the reduction of V. M can be also reduced by increasing D (Equation 14). Both M and C_D tend to decrease with the increase of D, but their dependences on D are weaker than their dependences on I, which leads to opposite effects: M tends to increase with I (Equation 13), while C_D decreases with I (Equation 12).

Equations 11and 12 show a strong correlation between the EIIs and the parameter I (high values of the $S_{X,Y}$), suggesting that they could be a suitable means for a rapid estimation of V and C_D, based only on I. Equations 13 and 14, instead, show a weaker correlation between M and the parameters I and D, suggesting that they would allow obtaining only a preliminary estimation of M, which is also affected by other parameters.

Given the conflicting effects that the modification of the degree of imperviousness of the catchment and the dilution coefficient of the CSO structure would have on the EIIs and the WTP operation, the choice of interventions aiming at reducing CSO pollution should consider both the sensitivity of the receiving water body and WTP operation issues. For instance, the WTP biological processes may be disrupted by higher (and more diluted) volumes conveyed, and additional costs would be required to process those additional volumes. So, the choice of modifications of I and D must be a trade-off between short-term and long-term environmental impacts on water bodies, and WTP operation efficiency and costs.

To verify the suitability of the proposed approach to real case studies,

Table 5
Equations of the fitting lines (see Fig. 7) of the most significant relationships linking controllable parameters and the EIIs, sorted by their $|S_{X,Y}|$ value.

Relationship		$S_{X,Y}$ value
$V = 4.70\, I^{1.08}$	(11)	$S_{I,V} = 0.82$
$C_D = 460\, I^{-0.39}$	(12)	$S_{I,C_D} = -0.71$
$M = 3835\, I^{0.39}$	(13)	$S_{I,M} = 0.56$
$M = 31857\, D^{-0.31}$	(14)	$S_{D,M} = -0.44$

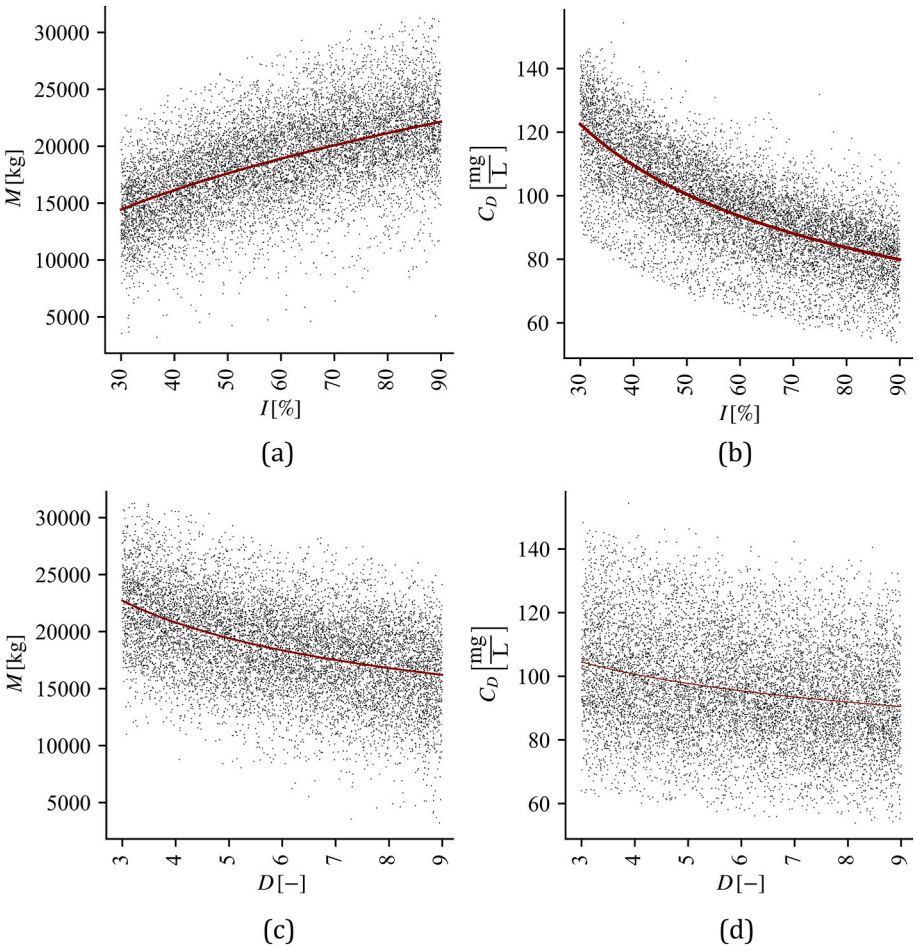

Fig. 9. Influence of the percentage of impervious surface, I, and the dilution coefficient, D, on the discharged pollutant mass, M, and the overflow pollutant concentration, C_D.

in Section 4.2 an application of the sensitivity analysis results to a real catchment in Portici (Fig. 4) is presented.

4.1. Considerations about CSO regulation

Many European Countries enforce regulations on the dilution coefficient, D (Zabel et al., 2001), and/or on the frequency of overflows, F (Botturi et al., 2021). However, this study showed that D, although being a *controllable* variable along with the percentage of impervious surface, I, does not strongly affect any of the indicators, EIIs. Indeed, D showed a moderate influence only on the discharged pollutant mass, M ($S_{D,M} = -0.44$) (Equation 14), comparable (but opposite) to the influence of I on M ($S_{I,M} = 0.56$) (Equation 13). This suggests that increasing D could be useful, but decreasing I is more important to reduce M. However, the reduction of I also leads to an increase of C_D (Equation 12), due to the reduction of the discharged volume, V (Equation 11). Thus, the choice of the most suitable values of the percentage of imperviousness and the dilution coefficient, must be a compromise between the containment of long-term pollution, related to the cumulated pollutant mass discharged, and the containment of short-term pollution, related to the concentration of pollutant in the overflow.

The scatter plots of the first row of Fig. 7 show that F is sensitive mostly to the nonlinear reservoir constant, α, which is a hardly *controllable* parameter, and secondarily to the yearly rainfall depth, R_D, which is a *non-controllable* parameter. A possible way to reduce α, and then F, not explored in this study, could be the installation of detention basins, that would smoothen the hydrograph at the outlet of the urban catchment, UC. Anyway, among all the EIIs, F resulted only moderately correlated with M (Fig. 6). The scatter plot of F and M (Fig. 10) shows that most of the dots gather in the range of F between 70 and 110 CSOs per year, thus reducing even further the significance of this relationship. Even if F was *controllable*, its regulation does not seem to be an effective strategy to address CSO pollution reduction.

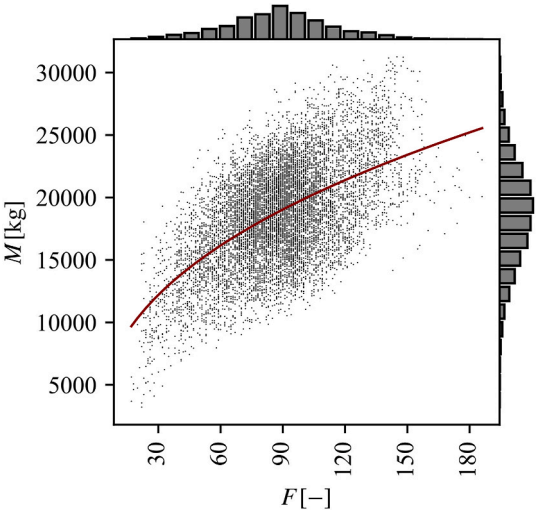

Fig. 10. Correlation between the frequency of CSOs, F, and the discharged pollutant mass, M. The red line is a power-law fitting curve.

4.2. CSO reduction strategies and case study application

The *non-controllable* parameters (Section 3.2) could be useful as initial information to estimate site-specific CSO variability. To provide a practical example, the variability of V, M, and C_D, towards I, was estimated for an UC belonging to the UDS of Portici, with $A = 1\,\text{km}^2$ (Fig. 4). Known characteristics of the UC were: the population density $5500\,\frac{\text{p}}{\text{km}^2}$, leading to a wastewater production per unit area $V_W = 400$ mm; the nonlinear reservoir constant $\alpha = 0.035\,\frac{m^{-\frac{2}{3}}}{s}$, obtained by estimating the width, W, and the average slope, s, based on topographic maps, and the Manning coefficient, n, from technical literature (Farina et al., 2023). The considered one-year rainfall time series had $R_D = 976$ mm (corresponding to the median yearly rainfall of the time series of the rain gauge of Ercolano), a maximum daily rainfall of 53 mm, a maximum intensity of $65\,\frac{\text{mm}}{\text{hr}}$, and 115 rainy days.

Fig. 11 shows the variability of V, M, and C_D, plotted against variations of I between 30% and 90%. It resulted:

- V varying in the range $[153; 700]$ mm ($S_{I,V} = 0.98$).
- M varying in the range $[11151; 24815]$ kg ($S_{I,M} = 0.76$).
- C_D varying in the range $[68; 114]\,\frac{\text{mg}}{\text{L}}$ ($S_{I,C_D} = -0.98$).

If also an estimation of I for the UC was available, then V, M, and C_D could be estimated through the red lines of Fig. 11, that fit the X, Y points of the relationships with I, respectively in panels a), b), and c). The remaining variability (the scatter of the dots around the fitting lines) is attributable to possible different choices of D.

Minimising M, and/or C_D could be an effective strategy to reduce the CSO impact, rather than targeting F, D, or V. Indeed, as shown before:

- F does not seem to be a good indicator of CSO environmental impact.
- D is less important than I, in terms of influence on the EIIs, and it also has a conflicting effect on M and the volume conveyed to the WTP, V_{WTP}, decreasing the former but increasing the latter.
- V does not carry information about pollution, even if it remains an important EII for the assessment of V_{WTP} for WTP design and evaluation of its operational costs.

M can be limited by reducing I, and/or increasing D. For example (see Fig. 12), if the initial I and D were $I = 70\%$, and $D = 5$, a 20% reduction of I would reduce M by 9%, from 20600 kg to 18700 kg, while a simultaneous increase of D from 5 to 8 would additionally reduce M by 16.5%, from 18700 kg to 15600 kg, for a total reduction of 24%. Additionally, while the 20% reduction of I alone, would increase C_D by 14%, from $79\,\frac{\text{mg}}{\text{L}}$ to $90\,\frac{\text{mg}}{\text{L}}$, the simultaneous increase of D from 5 to 8, would reduce C_D by 2%, from $90\,\frac{\text{mg}}{\text{L}}$ to $88\,\frac{\text{mg}}{\text{L}}$, so to contain the total increment to 11.5%.

As a result, the choice of reducing I and increasing D should consider the sensitivity of the water body in which CSOs are discharged: pollutant mass accumulation over time, or discharges with high pollutant concentration, may harm water bodies differently. Also, those choices may affect the WTP: changes in conveyed volumes, pollutant concentration and mass may alter the WTP operation, if opportune decisions are not adopted.

For example (Fig. 13), the 20% reduction of I, alone, would decrease V_{WTP}, by 2.5%, from 504 mm to 491 mm, while parallelly increasing D from 5 to 8 would increase V_{WTP} by 8.5%, from 491 mm to 533 mm, so that the combined effect would be a 5.5% increment.

To summarise, a hypothetical intervention consisting in a 20% reduction of the impervious surfaces, and a CSO structure modification to increase the dilution threshold from 5 to 8, would result in a 24% reduction of the yearly discharged mass, also leading to a 11.5% increase of the concentration of pollutant in the overflow, and a 5.5% increase of the volume conveyed to the WTP.

It is worth noting, again, that the 24% reduction of M, also comes with a 11.5% increase of C_D. Also, the balance between environmental benefits and required costs needs to be considered. In fact, the re-setting of the CSO structure activation threshold is a rapid and low-cost work, and it allows reducing C_D, but it also increases V_{WTP}. Additional energy costs would also be required if pumping stations are needed at the WTP. Differently, reducing I may have higher costs and work execution times (to remove impervious pavements and install porous ones), but this does not require additional capacity (and so adaptation costs) at the WTP, because they imply a reduction of both conveyed volume and pollutant mass.

5. Conclusions

This study investigates the variability of Combined Sewer Overflows (CSOs), described by environmental impact indicators (EIIs), through a Sensitivity Analysis (SA). The EIIs were analysed towards parameters characterising the local rainfall, the urban catchment, and the dilution activation threshold, D, of the CSO structure. A large sample of parameter sets (10000 examples) was investigated, therefore this study aimed at covering wide ranges of case studies. Also, a real case study was investigated.

A simplified approached to model the Urban Drainage System (UDS), the CSO structure and the water quality was implemented in the Storm Water Management Model (SWMM). This approach is suitable to obtain estimates of the overall pollution caused by CSOs over long periods of time (i.e., at yearly scale). Then, parameters and EIIs of relevance were identified, for which the SA was conducted: relationships were identified between the input parameters and the output parameters (EIIs).

The parameters were the rainfall depth, R_D; the wastewater production, V_W; the percentage of impervious surface of the urban catchment, I; the nonlinear reservoir constant of the urban catchment, α; the dilution threshold for the CSO structure, D. The EIIs were the frequency

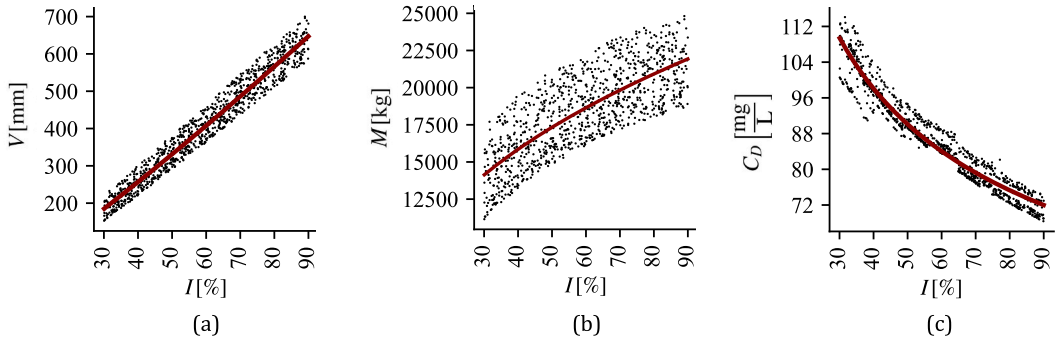

Fig. 11. V (a), M (b), and C_D (c), for an UC in Portici (Italy) with density of population $5500\,\frac{p}{km^2}$, $\alpha = 0.035\,\frac{m^{-\frac{2}{3}}}{s}$, and $R_D = 966\,mm$. The scatter of the dots around the fitting lines is due to the variability of D.

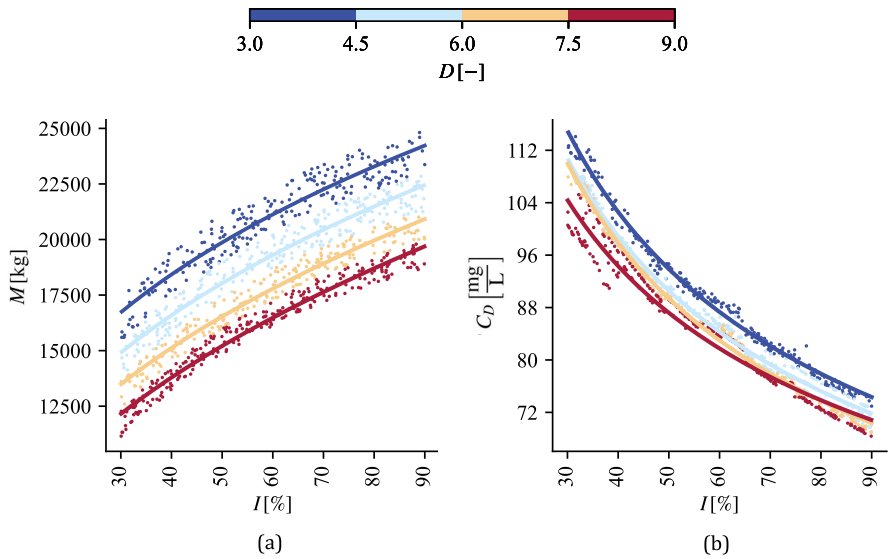

Fig. 12. Influence of the percentage of impervious surface, I, and the dilution coefficient, D (represented through different colors), on the discharged pollutant mass, M (a) and the overflow pollutant concentration, C_D (b), at yearly scale.

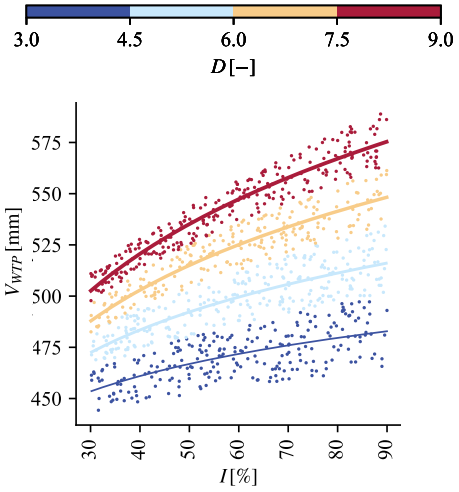

Fig. 13. Influence of I and D (represented through different colors), on V_{WTP}, at yearly scale.

of CSOs, F; the discharged volume, V; the discharged pollutant mass, M; the average pollutant concentration, C_D.

The results show that the percentage of impervious surface was the most influent parameter: in fact, the variability of the EIIs mostly depended on I. Also D showed some influence on the EIIs, although its effects were smaller than those of I.

More precisely, reducing the imperviousness can lead to a significant reduction of discharged pollutant mass and volume, but also to an increment of the pollutant concentration in the overflows. For this reason, aiming at pollutant load reduction, it is useful to reduce the impervious surfaces, but this should be made considering the condition of the water body and the desired target of environmental remediation. However, to contain C_D, an increment of D may be of help: on the other hand, this leads to increased wastewater treatment plant (WTP) influent volume, V_{WTP}, with growing costs of WTP operation. Hence, the trade-off between environmental benefits and increased costs, should also be considered when designing CSO reduction strategies.

The wide range of the investigated parameters supported these considerations, and it allowed to identify four significant relationships between parameters and EIIs, which equations may be useful to: estimate the indicators in urban environments with known characteristics; design CSO pollution reduction strategies, based on target values of M and/or C_D.

Current CSO regulations in Europe often pose limits on F: however, in this study, F was found to be barely *controllable*, and uncorrelated to any of the other EIIs, indicating that its regulation is not an effective strategy to reduce CSOs. Regulations also enforce fixed values for D, which, however, was found to be less important than I in reducing CSO pollution.

The results of this study can thus support the improvement of CSO regulation, by shifting focus from fixed criteria to indicator-based criteria. It needs to be noted that, since simplified hypotheses on water quality modelling were adopted, the relationships do not claim to be accurate, rather they are useful to guide the design of interventions when no accurate CSO quantity and quality measurements are available. The methodology presented is suitable to be applied to any pollutant, adjusting the water quality model parameters accordingly.

Additional data

All data and files used in the study are available at the relevant given references or upon reasonable request.

The computer configuration used in this study was: OS Windows 11 64-bit, CPU AMD Ryzen 5 4500U, RAM 24 GB. The software configuration used in this study was: Python 3.11.4, EPA-SWMM 5.2.3, swmm-api 0.4.26.

Funding

This study was funded by INPS (Det. n. 431 of November 09, 2020, https://www.inps.it/news/dottorati-di-ricerca-2019-20-pubblicato-il-bando), as part of the Ph.D. project “Sustainability of the integrated water cycle with reference to the impact of overflows on the environmental quality” within the Doctoral Course “A.D.I.” of Università degli Studi della Campania “L. Vanvitelli” in partnership with GORI S.p.A.

CRediT authorship contribution statement

Alessandro Farina: Writing - review & editing, Writing - original

draft, Validation, Software, Methodology, Investigation, Data curation. **Rudy Gargano:** Writing - review & editing, Validation, Supervision, Methodology, Conceptualization. **Roberto Greco:** Writing - review & editing, Validation, Supervision, Methodology, Funding acquisition, Conceptualization.

Declaration of competing interest

The authors declare that they have no known competing financial interests or personal relationships that could have appeared to influence the work reported in this paper.

Data availability

Data will be made available on request.

List of Acronyms and Symbols

α	Nonlinear reservoir constant
σ	Standard deviation
A	Area of the catchment
b	Pollutant buildup
BOD_5	Biochemical Oxygen Demand after five days
$C1$	Maximum pollutant build-up
$C2$	Pollutant buildup rate constant
$C3$	Wash-off coefficient
$C4$	Wash-off exponent
C_D	Pollutant concentration in the combined sewer overflow
C_R	Pollutant concentration in stormwater
C_W	Pollutant concentration in wastewater
C_{WTP}	Pollutant concentration in the flow conveyed to the wastewater treatment plant
cov	Covariance
CSO	Combined Sewer Overflow
Δt	Resolution of timeseries
ΔT	Period of time
D	Dilution activation threshold of the combined sewer overflow structure
d	Depth of water accumulated on the surface
d_s	Depression storages of the surface of the catchment
EII	Environmental impact indicator
F	Frequency of combined sewer overflows
f^W	Shape coefficient of the catchment
I	Percentage of impervious surface of the catchment
M	Pollutant mass discharged
N	Number of timesteps per timeseries
n	Manning roughness coefficient
Q	Sewer flow
Q_D	Flow discharged by the combined sewer overflow
Q_R	Runoff of the catchment
Q_W	Wastewater discharge
Q_{WTP}	Flow conveyed to the wastewater treatment plant
q	Runoff per unit area of the catchment
r	Rank
R_D	Yearly cumulated rain
$S_{X,Y}$	Spearman rank correlation coefficient of the X input and Y output
s	Slope of the catchment
SA	Sensitivity Analysis
SWMM	Storm Water Management Model
t_b	Antecedent dry weather days
t_w	Days from the beginning of the wash-off
TSS	Total Suspended Solids
UC	Urban Catchment
UDS	Urban Drainage System
V	Discharged volume
V_W	Wastewater production per unit area of the catchment
V_{WTP}	Volume conveyed to the wastewater treatment plant
W	Width of the catchment
w	Pollutant wash-off
WTP	Wastewater Treatment Plant
X	Generic input variable of the sensitivity analysis
Y	Generic output variable of the sensitivity analysis

References

Barco, J., Papiri, S., Stenstrom, M.K., 2008. First flush in a combined sewer system. Chemosphere 71 (5), 827–833. https://doi.org/10.1016/j.chemosphere.2007.11.049.

Botturi, A., Ozbayram, E.G., Tondera, K., Gilbert, N.I., Rouault, P., Caradot, N., Gutierrez, O., Daneshgar, S., Frison, N., Akyol, Ç., Foglia, A., Eusebi, A.L., Fatone, F., 2021. Combined sewer overflows: a critical review on best practice and innovative solutions to mitigate impacts on environment and human health. Crit. Rev. Environ. Sci. Technol. 51 (15), 1585–1618. https://doi.org/10.1080/10643389.2020.1757957.

Butler, D., Digman, C.J., Makropoulos, C., Davies, J.W., 2018. Urban drainage. In: Urban Drainage, Fourth Edition, fourth ed. CRC Press. https://doi.org/10.1201/9781351174305.

Chen, C.W., Shubinski, R.P., 1971. Computer simulation of urban storm water runoff. J. Hydraul. Div. 97 (2), 289–301. https://doi.org/10.1061/JYCEAJ.0002871.

Di Nunno, F., Granata, F., Parrino, F., Gargano, R., de Marinis, G., 2021. Microplastics in combined sewer overflows: an experimental study. J. Mar. Sci. Eng. 9 (12), 1415. https://doi.org/10.3390/jmse9121415.

Dirckx, G., Fenu, A., Wambecq, T., Kroll, S., Weemaes, M., 2019. Dilution of sewage: is it, after all, really worth the bother? J. Hydrol. 571, 437–447. https://doi.org/10.1016/J.JHYDROL.2019.01.065.

Dirckx, G., Thoeye, C., De Gueldre, G., Van De Steene, B., 2011. CSO management from an operator's perspective: a step-wise action plan. Water Sci. Technol. 63 (5), 1044–1052. https://doi.org/10.2166/wst.2011.288.

Dirckx, G., Vinck, E., Kroll, S., 2022. Stochastic determination of combined sewer overflow loads for decision-making purposes and operational follow-up. Water 2022 14 (10), 1635. https://doi.org/10.3390/W14101635. Page 1635, 14.

DPCN, 2023. Export Archivio Dati Per Sensore. http://centrofunzionale.regione.campania.it/#/pages/sensori/sensor-utility.

Engelhard, C., De Toffol, S., Rauch, W., 2008. Suitability of CSO performance indicators for compliance with ambient water quality targets. Urban Water J. 5 (1), 43–49. https://doi.org/10.1080/15730620701736902.

Eulogi, M., Ostojin, S., Skipworth, P., Kroll, S., Shucksmith, J.D., Schellart, A., 2022. Optimal positioning of RTC actuators and SuDS for sewer overflow mitigation in urban drainage systems. Water 14 (23), 3839. https://doi.org/10.3390/W14233839, 2022, Vol. 14, Page 3839.

Farina, A., Di Nardo, A., Gargano, R., Greco, R., 2022. Assessing the environmental impact of combined sewer overflows through a parametric study. EWaS5 19, 8. https://doi.org/10.3390/environsciproc2022021008.

Farina, A., Di Nardo, A., Gargano, R., van der Werf, J.A., Greco, R., 2023. A simplified approach for the hydrological simulation of Urban Drainage Systems with SWMM. J. Hydrol., 129757 https://doi.org/10.1016/J.JHYDROL.2023.129757.

Ferraro, A., de Sario, S., Attanasio, A., Di Capua, F., Gorgoglione, A., Fratino, U., Mascolo, M.C., Pirozzi, F., Trancone, G., Spasiano, D., 2023. Phosphorus recovery as struvite and hydroxyapatite from the liquid fraction of municipal sewage sludge with limited magnesium addition. J. Environ. Qual. 52 (3), 584–595. https://doi.org/10.1002/JEQ2.20446.

Giakoumis, T., Voulvoulis, N., 2023. Combined sewer overflows: relating event duration monitoring data to wastewater systems' capacity in England. Environ. Sci.: Water Research & Technology 9 (3), 707–722. https://doi.org/10.1039/D2EW00637E.

Gupta, K., Saul, A.J., 1996. Specific relationships for the first flush load in combined sewer flows. Water Res. 30 (5), 1244–1252. https://doi.org/10.1016/0043-1354(95)00282-0.

Hossain, I., Imteaz, Dr M., Gato-Trinidad, Dr S., Shanableh, Prof A., 2010. Development of a Catchment Water Quality Model for Continuous Simulations of Pollutants Build-Up and Wash-Off. https://doi.org/10.5281/ZENODO.1084178.

Inc. Metcalf & Eddy, 2013. Wastewater Engineering: Treatment and Resource Recovery, Ed.; 5th ed. McGraw Hill https://www.mheducation.com/highered/product/wastewater-engineering-treatment-resource-recovery-metcalf-eddy-inc-tchobanoglous/M9780073401188.html.

Jensen, D.M.R., Sandoval, S., Aubin, J.B., Bertrand-Krajewski, J.L., Xuyong, L., Mikkelsen, P.S., Vezzaro, L., 2022. Classifying pollutant flush signals in stormwater using functional data analysis on TSS MV curves. Water Res. 217, 118394 https://doi.org/10.1016/J.WATRES.2022.118394.

Jia, Y., Zheng, F., Maier, H.R., Ostfeld, A., Creaco, E., Savic, D., Langeveld, J., Kapelan, Z., 2021. Water quality modeling in sewer networks: review and future research directions. Water Res. 202, 117419 https://doi.org/10.1016/j.watres.2021.117419.

Joshi, P., Leitão, J.P., Maurer, M., Bach, P.M., 2021. Not all SuDS are created equal: impact of different approaches on combined sewer overflows. Water Res. 191, 116780 https://doi.org/10.1016/J.WATRES.2020.116780.

Lucas, W.C., Sample, D.J., 2015. Reducing combined sewer overflows by using outlet controls for Green Stormwater Infrastructure: case study in Richmond, Virginia. J. Hydrol. 520, 473–488. https://doi.org/10.1016/J.JHYDROL.2014.10.029.

Luo, H., Luo, L., Huang, G., Liu, P., Li, J., Hu, S., Wang, F., Xu, R., Huang, X., 2009. Total pollution effect of urban surface runoff. J. Environ. Sci. 21 (9), 1186–1193. https://doi.org/10.1016/S1001-0742(08)62402-X.

Mallin, M.A., Johnson, V.L., Ensign, S.H., 2009. Comparative impacts of stormwater runoff on water quality of an urban, a suburban, and a rural stream. Environ. Monit. Assess. 159 (1–4), 475–491. https://doi.org/10.1007/s10661-008-0644-4.

Mamun, A. Al, Shams, S., Nuruzzaman, M., 2020. Review on uncertainty of the first-flush phenomenon in diffuse pollution control. Appl. Water Sci. 10 (1), 1–10. https://doi.org/10.1007/s13201-019-1127-1.

Maniquiz-Redillas, M., Robles, M.E., Cruz, G., Reyes, N.J., Kim, L.H., 2022. First flush stormwater runoff in urban catchments: a bibliometric and comprehensive review. Hydrology 9 (4), 1–22. https://doi.org/10.3390/hydrology9040063.

McGinnis, S.M., Burch, T., Murphy, H.M., 2022. Assessing the risk of acute gastrointestinal illness (AGI) acquired through recreational exposure to combined sewer overflow-impacted waters in Philadelphia: A quantitative microbial risk assessment. Microbial Risk Analysis 20, 100189. https://doi.org/10.1016/J.MRAN.2021.100189.

Munro, K., Martins, C.P.B., Loewenthal, M., Comber, S., Cowan, D.A., Pereira, L., Barron, L.P., 2019. Evaluation of combined sewer overflow impacts on short-term pharmaceutical and illicit drug occurrence in a heavily urbanised tidal river catchment (London, UK). Sci. Total Environ. 657, 1099–1111. https://doi.org/10.1016/J.SCITOTENV.2018.12.108.

Nasrabadi, T., Ruegner, H., Sirdari, Z.Z., Schwientek, M., Grathwohl, P., 2016. Using total suspended solids (TSS) and turbidity as proxies for evaluation of metal transport in river water. Appl. Geochem. 68, 1–9. https://doi.org/10.1016/J.APGEOCHEM.2016.03.003.

Nazahiyah, R., Yusop, Z., Abustan, I., 2007. Stormwater quality and pollution loading from an urban residential catchment in Johor, Malaysia. Water Sci. Technol. 56 (7), 1–9. https://doi.org/10.2166/WST.2007.692.

Nickel, J.P., Fuchs, S., 2019. Micropollutant emissions from combined sewer overflows. Water Sci. Technol. 80 (11), 2179–2190. https://doi.org/10.2166/WST.2020.035.

Petrie, B., 2021. A review of combined sewer overflows as a source of wastewater-derived emerging contaminants in the environment and their management. Environ. Sci. Pollut. Control Ser. 28 (25), 32095–32110. https://doi.org/10.1007/s11356-021-14103-1.

Pichler, M., 2022. Swmm-Api: API for Reading, Manipulating and Running SWMM-Projects with python. https://doi.org/10.5281/zenodo.5862140.

Pistocchi, A., 2020. A preliminary pan-European assessment of pollution loads from urban runoff. Environ. Res. 182 https://doi.org/10.1016/J.ENVRES.2020.109129.

Quaranta, E., Fuchs, S., Liefting, H.J., Schellart, A., Pistocchi, A., 2022. Costs and benefits of combined sewer overflow management strategies at the European scale. J. Environ. Manag. 318 https://doi.org/10.1016/J.JENVMAN.2022.115629, 115629–115629.

Romero, L., Joseph-Duran, B., Sun, C., Meseguer, J., Cembrano, G., Guasch, R., Martínez, M., Muñoz, E., Puig, V., 2021. An integrated software architecture for the pollution-based real-time control of urban drainage systems. J. Hydroinf. 23 (3), 671–687. https://doi.org/10.2166/HYDRO.2021.149.

Rossman, L.A., Huber, W.C., 2016a. Storm Water Management Model Reference Manual Volume I – Hydrology, vol. I. U.S. Environmental Protection Agency (January), 231. https://www.epa.gov/water-research/storm-water-management-model-swmm.

Rossman, L.A., Huber, W.C., 2016b. Storm Water Management Model Reference Manual Volume III - Water Quality. U.S. EPA Office of Research and Development, Washington, DC. EPA/600/R-16/093, III(January), 231. https://www.epa.gov/water-research/storm-water-management-model-swmm.

Saltelli, A., Annoni, P., Azzini, I., Campolongo, F., Ratto, M., Tarantola, S., 2010. Variance based sensitivity analysis of model output. Design and estimator for the total sensitivity index. Comput. Phys. Commun. 181 (2), 259–270. https://doi.org/10.1016/J.CPC.2009.09.018.

Saltelli, A., Ratto, M., Andres, T., Campolongo, F., Cariboni, J., Gatelli, D., Saisana, M., Tarantola, S., 2008. Global sensitivity analysis: the primer. Global Sensitivity Analysis: The Primer 1–292. https://doi.org/10.1002/9780470725184.

Sandoval, S., Torres, A., Pawlowsky-Reusing, E., Riechel, M., Caradot, N., 2013. The evaluation of rainfall influence on combined sewer overflows characteristics: the Berlin case study. Water Sci. Technol. 68 (12), 2683–2690. https://doi.org/10.2166/WST.2013.524.

Sawyer, C.N., McCarty, P.L., Parkin, G.F., 2003. Chemistry for Environmental Engineering and Science, 5th (edn. McGraw-Hill Inc, New York. https://www.worldcat.org/title/49285370.

Schellart, A., Bertrand-Krajewski, J.-L., Rieckermann, J., Tait, S., 2023. How to Monitor and Regulate Combined Sewer Overflows? Novatech 2023. GRAIE. https://hal.science/hal-04162425.

Schroeder, K., Riechel, M., Matzinger, A., Rouault, P., Sonnenberg, H., Pawlowsky-Reusing, E., Gnirss, R., 2011. Evaluation of effectiveness of combined sewer overflow control measures by operational data. Water Sci. Technol. 63 (2), 325–330. https://doi.org/10.2166/WST.2011.058.

Seco, I., Schellart, A., Gómez-Valentín, M., Tait, S., 2018. Prediction of organic combined sewer sediment release and transport. J. Hydraul. Eng. 144 (3), 04018003 https://doi.org/10.1061/(ASCE)HY.1943-7900.0001422.

Seidl, M., Servais, P., Mouchel, J.M., 1998. Organic matter transport and degradation in the river Seine (France) after a combined sewer overflow. Water Res. 32 (12), 3569–3580. https://doi.org/10.1016/S0043-1354(98)00169-9.

Sojobi, A.O., Zayed, T., 2022. Impact of sewer overflow on public health: a comprehensive scientometric analysis and systematic review. Environ. Res. 203 (April 2021), 111609 https://doi.org/10.1016/j.envres.2021.111609.

Torres, M.N., Rabideau, A., Ghodsi, S.H., Zhu, Z., Shawn Matott, L., 2022. Spatial design strategies and performance of porous pavements for reducing combined sewer overflows. J. Hydrol. 607 https://doi.org/10.1016/j.jhydrol.2022.127465.

Trancone, G., Spasiano, D., Race, M., Luongo, V., Petrella, A., Pirozzi, F., Fratino, U., Piccinni, A.F., 2022. A combined system for asbestos-cement waste degradation by dark fermentation and resulting supernatant valorization in anaerobic digestion. Chemosphere 300, 134500. https://doi.org/10.1016/J.CHEMOSPHERE.2022.134500.

Tu, M.C., Smith, P., 2018. Modeling pollutant buildup and washoff parameters for SWMM based on land use in a semiarid urban watershed. Water Air Soil Pollut. 229 (4), 1–15. https://doi.org/10.1007/s11270-018-3777-2.

Vezzaro, L., 2021. Extrapolating performance indicators for annual overflow volume reduction of system-wide real time control strategies 19 (1), 15–21. https://doi.org/10.1080/1573062X.2021.1948078.

Wicke, D., Cochrane, T.A., O'Sullivan, A., 2012. Build-up dynamics of heavy metals deposited on impermeable urban surfaces. J. Environ. Manag. 113, 347–354. https://doi.org/10.1016/J.JENVMAN.2012.09.005.

Xu, Z., Wu, J., Li, H., Chen, Y., Xu, J., Xiong, L., Zhang, J., 2018. Characterizing heavy metals in combined sewer overflows and its influence on microbial diversity. Sci. Total Environ. 625, 1272–1282. https://doi.org/10.1016/J.SCITOTENV.2017.12.338.

Yaranal, N.A., Kuchibhotla, S.A., Subbiah, S., Mohanty, K., 2023. Identification, removal of microplastics and surfactants from laundry wastewater using electrocoagulation method. Water Emerging Contaminants & Nanoplastics 3 (1). https://doi.org/10.20517/WECN.2023.46.

Zabel, T., Milne, I., Mckay, G., 2001. Approaches adopted by the European Union and selected Member States for the control of urban pollution. Urban Water 3 (1–2), 25–32. https://doi.org/10.1016/S1462-0758(01)00019-X.

Zeng, J., Huang, G., Luo, H., Mai, Y., Wu, H., 2019. First flush of non-point source pollution and hydrological effects of LID in a Guangzhou community. Scientific Reports 2019 9:1 9 (1), 1–10. https://doi.org/10.1038/s41598-019-50467-8.

Zhang, Z., Tian, W., Liao, Z., 2023. Towards coordinated and robust real-time control: a decentralized approach for combined sewer overflow and urban flooding reduction based on multi-agent reinforcement learning. Water Res. 229, 119498 https://doi.org/10.1016/J.WATRES.2022.119498.